Sigma J Eng Nat Sci, Vol. 44, No. 2, pp. 1127–1137, April, 2026

Sigma Journal of Engineering and Natural Sciences
Web page info: https://sigma.yildiz.edu.tr
DOI: 10.14744/sigma.2026.2031

Research Article

Dynamic mechanical, morphological, and thermal characteristics of polypropylene/red mud polymer composites

Beril EKER[1,*], Özlem YAĞCI[2], Elif ULUTAŞ[3], Munir TAŞDEMIR[3], Volkan Murat YILMAZ[4]

[1]*Science and Technology Application and Research Center, Yıldız Technical University, Istanbul, 34220, Türkiye*
[2]*Department of Physics, Yildiz Technical University, Istanbul, 34220, Türkiye*
[3]*Department of Metallurgical and Materials Engineering, Faculty of Technology, Marmara University, Istanbul, 34722, Türkiye*
[4]*Central Research Laboratory Research & Application Center, Bartın University, Bartın, 74100, Türkiye*

ARTICLE INFO

Article history
Received: 03 November 2025
Revised: 12 January 2026
Accepted: 14 February 2026

Keywords:
Composites; Polypropylene; Red Mud; Storage Modulus; Thermal Properties

ABSTRACT

This study aims to examine how different amounts of red mud (RM) (0, 10, 20, 30, and 40 wt.%) affect the dynamic mechanical and thermal characteristics of polypropylene (PP)/red mud (RM) polymer composites. Fourier Transform Infrared Spectroscopy (FTIR) was used to confirm the presence of PP and RM in the samples. The distribution of RM in the PP matrix was analysed using Scanning Electron Microscopy (SEM). X-ray Diffraction (XRD) results showed that crystallinity of polypropylene increased from 80.04% for pure PP to 94.94% for the composite containing 40 wt% red mud. Thermogravimetric Analysis (TGA) was employed to analyse the thermal stability of the polypropylene (PP)/red mud (RM) polymer composites. Specifically, it was used to assess the thermal stability of the composites, with results indicating excellent stability for the 40 wt.% RM composites. Differential Scanning Calorimetry (DSC) was used to compare the melting temperatures (Tm) of the composites. There is a slight increase in Tm, from 169.08 °C for pure polypropylene to 171.45 °C for the composite with 40 wt% red mud. Furthermore, Dynamic Mechanical Analysis (DMA) results revealed a 58% reduction from the storage modulus of the pure polypropylene (6.28×10^8 Pa) to the storage modulus of the composite containing 40 wt% red mud (2.60×10^8 Pa).
The research highlights that red mud (RM) waste is a low-cost, sustainable filler material in a polypropylene matrix. It enhances thermal stability and structural performance for various engineering applications.

Cite this article as: Eker B, Yağcı Ö, Ulutaş E, Taşdemir M, Yılmaz VM. Dynamic mechanical, morphological, and thermal characteristics of polypropylene/red mud polymer composites. Sigma J Eng Nat Sci 2026;44(2):1127–1137.

***Corresponding author.**
*E-mail address: beker@yildiz.edu.tr

This paper was recommended for publication in revised form by Editor-in-Chief Ahmet Selim Dalkilic

Published by Yıldız Technical University Press, İstanbul, Turkey

INTRODUCTION

The demand for eco-friendly polymers and polymer composites derived from renewable resources is increasing. Growing environmental concerns and the depletion of fossil resources drive this demand. The use of waste materials has gained increasing attention due to their advantages from both environmental and economic perspectives. The chemical composition of red mud is 37.67% Fe_2O_3, 5.55% TiO_2, 20.42% Al_2O_3. Red mud has reddish-brown colouration and a very fine grain size. The characteristic fine grains of red mud favour its use as an admixture in mortar and concrete. The mineralogical composition of red mud varies with the bauxite source and production method.

Red mud is a waste byproduct produced during the extraction of alumina from bauxite through the Bayer process. Acidic, electrothermic, and basic methods are used for alumina production. The demand for alumina has increased with global Al consumption. For one tonne of alumina or 0.5 tonnes of aluminium metal produced, approximately one tonne of red mud is generated. Red mud is the most significant waste issue in this industry due to the increasing production of aluminium. Between 120 and 150 million tons of red mud are produced annually [1]. Disposing of red mud is challenging due to its toxicity and high alkalinity. Red mud is a byproduct of aluminium production and contains hazardous substances, including heavy metals and radioactive materials. There are various disposal methods as follows: 1) Ocean dumping: the mud is released into coastal waters, 2) lagoons: storing the mud in large ponds, 3) dry stacking: the mud is stored in a dry form, 4) dry cake disposal: solidifying the mud before disposal [2]. As aluminium production increases, bauxite consumption and red mud generation also increase. The accumulation of red mud causes several environmental problems. Under hot, dry conditions, dried red mud particles can cause air pollution through wind dispersion. Moreover, red mud stored in dams or disposal sites may damage biological and ecological systems. Red mud is hazardous industrial waste composed of iron compounds and heavy metals. If disposal dams are not constructed and managed in compliance with applicable legislation and engineering standards, red mud will irreversibly harm living organisms and the environment. Therefore, the industrial utilization of red mud is a critical strategy to mitigate its environmental harm, and research into its safe and sustainable reuse is ongoing [3,4].

Red mud has been assessed in various industrial sectors, including building materials production [5,6], catalysis [7], as well as in the development of materials like metal and/or polymer matrix composites, geopolymers [8,9], iron, steel manufacturing [10], and ceramics [11].

With the utilization of red mud, environmental pollution will be prevented, the storage problem will be eliminated, the cost of aluminium production will be reduced, and an economic contribution will be provided to the metallurgy, construction and chemical industries. Red mud has various potential uses, such as an adsorbent, construction material, and pigment in the ceramics sector. It can additionally function as an absorbent for exhaust gases. Another possible use is the recovery of precious elements from red mud, including iron, aluminium, titanium, and rare-earth metals such as scandium, cerium, and lanthanum.

The first article on red mud was published in 1976, but research on this topic gained much attention only in 2010. Since then, the number of articles on red mud has increased rapidly. This rise is primarily due to environmental concerns about hazardous red mud and interest in adopting circular-economy practices to manage it. This upward trend is expected to persist because current research doesn't provide enough information to achieve full industrial utilisation of red mud. However, with further research, the full potential of red mud can be unlocked, inspiring a new era of sustainable waste management and circular economy practices [12].

Red mud can be added to polymer materials as a reinforcement and filler. In recent years, red mud has been incorporated into polymer materials, thereby expanding the use of newly developed blends. Red mud is a plentiful and low-cost reinforcing material for thermoplastics used in construction, electrical applications, decorative household applications, and the packaging industry [13].

Zhang et al.'s study reported that as the red mud content in PP-based composites increased, bending strength, tensile strength, heat deflection temperature, and Vicat softening point all improved, whereas shock resistance decreased. In their research, the PP composites reinforced with 15 wt% red mud exhibited the highest tensile strength [14].

Akıncı et al. investigated the impact of red mud content (10, 20, 30, 40, and 50 wt.%) on isotactic polypropylene/red mud composites in terms of tension, three-point bending, and hardness test results. Their findings indicated that as the red mud content increased, the composites' hardness improved, whereas bending strength, tensile strength, and elongation at failure decreased [15]. Most existing studies focus on either mechanical or thermal properties individually, often within a limited range of filler loadings [16,17]. Recent studies have also examined the tribological and microstructural performance of filler-matrix interaction and dispersion quality in terms of overall composite performance [18,19].

The originality of this study lies in the use of untreated red mud, an industrial waste by-product, as a filler in polypropylene matrix without surface modification or compatibilizers. Most previous studies focus on chemically treated red mud or systems designed for better dispersion. This work provides a direct evaluation of the effects of raw red mud on the morphological, mechanical, and thermomechanical properties of PP.

The main goal is to explore the potential use of waste RM as a low-cost and sustainable filler in PP matrix. The existing literature indicates that PP composites incorporating RM have primarily been examined for their limited mechanical or thermal properties. In contrast, this study systematically

investigates the combined effects of varying RM additions on the dynamic mechanical behaviour, crystalline structure, and thermal stability of the composites. In this context, the study aims not only to evaluate the effect of RM on the overall performance of PP composites but also to reveal the structure–property relationships through detailed analyses. This approach, based on recycling industrial waste, contributes to both reducing material costs and mitigating environmental impacts associated with RM storage. The results obtained are expected to enable RM to find broader applications in the development of high-performance polymer composites. Figure 1 shows graphical presentation of the study.

EXPERIMENTAL

Materials

The red mud was obtained from Güray Seramik Company in Avanos, Nevşehir, Turkey. The PP (Moplen EP 3307) was sourced from Lyondell Basell. It has a density of 0.900 g/cm^3, an MFI of 15 g/10 min (230°C, 2.16 kg), and a heat deflection temperature (0.45 MPa, unannealed) of 95.0°C.

Production of The Composites

The red mud was pre-dried at 85°C for 24 hours to break down associated hydrates. Then, Siemens Simatic C7-621 is used to produce powders. The particle size of the red mud ranged from 38 to 250 micrometres. Solid compositions were mechanically premixed with an LB-5601 liquid-solids batch blender for 15 minutes. The composites were produced using a Microsan extruder at temperatures of 170-220°C, a pressure of 25-30 bar, and a rotational speed of 23 rpm. Following extrusion, the polymer composites were dried in a vacuum oven at 80°C for 24 hours. Finally, test samples were produced using an injection moulding machine at temperatures of 170–220°C, a pressure of 90–120 bar, and a screw speed of 23 rpm.

Table 1 presents the percentages of polypropylene and red mud for each group.

Table 1. The makeup of the various polymer composite formulations.

Groups	PP (wt %)	Red Mud (RM) (wt %)
1	100	-
2	90	10
3	80	20
4	70	30
5	60	40

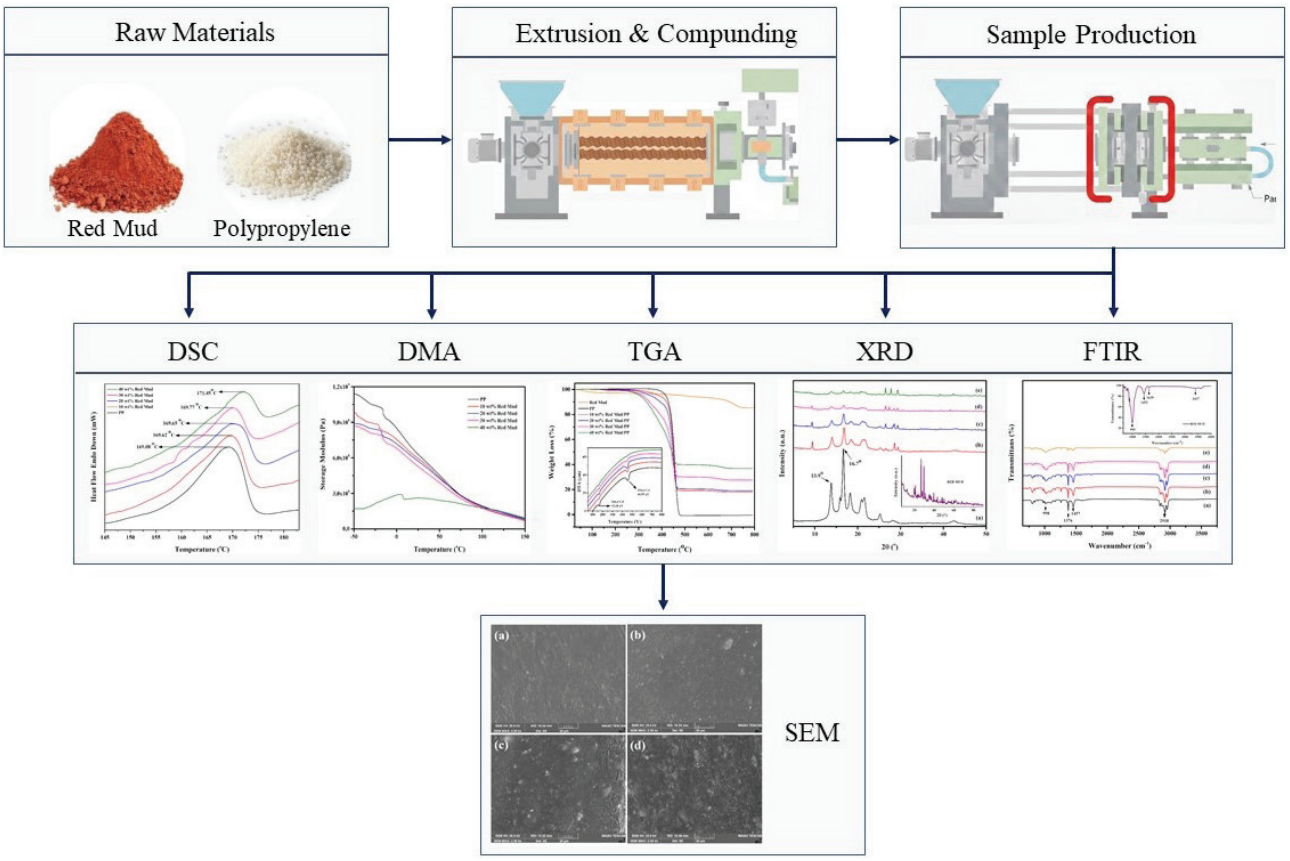

Figure 1. Graphical presentation of the study.

CHARACTERIZATION METHODS

Fourier Transform Infrared Analysis

The FTIR Spectrum 100 Perkin Elmer was utilized to analyze the samples in transmittance mode across a wavelength range of 600–4000 cm^{-1}.

Surface Morphology

The examination was conducted using an EVO LS Zeiss operating at 3 kV.

X-Ray Diffraction Examination

The measurements were carried out using a Panalytical X'PERT PRO X-ray diffractometer equipped with monochromatic CuKα radiation, functioning at 45 kV and 40 mA under ambient conditions.

Dynamic Mechanical Analysis

The DMA 8000 Perkin Elmer was employed for the analysis. The deformation mode used was single cantilever bending with a 50 µm amplitude, a frequency of 1 Hz, a heating rate of 5°C/min, and a temperature range of -50°C to 150°C.

Thermogravimetric Analysis

The EXSTAR TG/DTA 6300 Seiko device was employed for the assessments. Samples weighing 5-10 mg were placed in a platinum crucible under a nitrogen environment and heated from ambient temperature to 800°C at a rate of 10°C/min.

Differential Scanning Calorimetry Examination

The DSC evaluations of the samples (8±1 mg, n=5) were performed using a Perkin-Elmer Diamond DSC 8230 in a nitrogen atmosphere at a flow rate of 50 mL/min. The gathered data was then processed using Pyris Software. The specimens were heated at 10 °C/min over the 20–200 °C temperature range.

RESULTS AND DISCUSSION

Fourier Transform Infrared Analysis

FTIR spectroscopy uses infrared light to identify chemical bonds in molecules for organic and inorganic materials [20,21]. Thus, it enables the content of the tested sample to be determined. FTIR spectra of PP/RM composites blended in varying proportions (0-40 wt% RM) were shown in Figure 2.

The main transmittance bands observed in the FTIR spectrum in this study were consistent with those reported in the literature [22]. 2918 cm^{-1} (CH_2), 2951 cm^{-1} (CH_3), 2839 cm^{-1} (CH_2), 1457 cm^{-1} (CH_2), 1376 cm^{-1} (CH_3), 1359 cm^{-1} (CH_2- CH), 1330 cm^{-1} (CH_2- CH), 998 cm^{-1} (CH_3), 973 cm^{-1} (CH_3, C–C), 841cm^{-1} (C–H), 808 cm^{-1} (C–C), 1304 cm^{-1}, 1223 cm^{-1}, 1261 cm^{-1}, 1168 cm^{-1}, and 1154 cm^{-1} (CH_3), (CH_2), (CH), respectively. The intensity of the characteristic PP bands decreased as RM was mixed with PP in increasing proportions. In the FTIR spectrum of RM, the absorption bands were seen at 3437, 2920, 2853, 1745, 1639, 1578, 1560, 1542, 1452, 1402, 995, 802 and 654 cm^{-1}

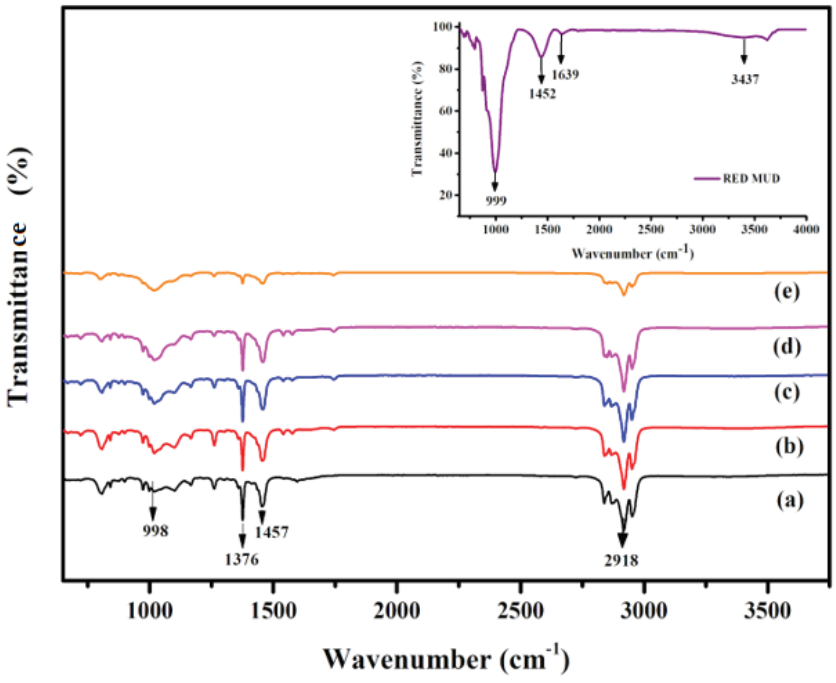

Figure 2. The FTIR spectra of (a) pure PP, (b) 10 wt%, (c) 20 wt%, (d) 30 wt%, (e) 40 wt% red mud powder mixed PP composites.

[23]. The band at 3437 cm^{-1} corresponds to an envelope of hydrogen-bonded surface OH groups. The bands at 2920 and 2853 cm^{-1} were assigned to the CH_2 symmetric or asymmetric stretch of the organic hydrocarbon compound in the red mud. The absorption band at 1745 cm^{-1} corresponds to the C=O double bond. The absorption band at 1639 cm^{-1} is attributed to the bending vibration of H-O-H from water in the structure of the aluminosilicate material. It is estimated that the band at 1452 cm^{-1} may be due to the carbonate component originating from calcite. The band at 999 cm^{-1} can be attributed to the stretching of the Si–O–Si bond [24-26]. FTIR measurements confirmed that RM was successfully incorporated into the PP matrix. The interaction between PP and RM is mainly physical.

Surface Morphology

Figure 3 shows the surfaces of PP/RM composites with different weight ratios (0, 10, 30, and 40 wt%) of RM. The images reveal that RM particle clusters are mixed into the PP, and as the amount of RM in the composite increases, there is an increase in the agglomeration of the powder (Figure 3b-d). The rise in RM concentration leads to the formation of agglomerates, thereby reducing the storage modulus. This result was confirmed by the SEM images, which supported the DMA result.

X-Ray Diffraction Examination

The XRD pattern of the RM, pure and 10 wt.%,20 wt.%, 30wt.% and 40 wt% red mud mixed PP matrix is given in Figure 4. It can be seen from the XRD pattern of RM, its composition is composed of many different components in accordance with the literature. From Figure 4, the main components of RM are Quartz (SiO_2), Dicalcium silicate (Ca_2SiO_4), Hematite (Fe_2O_3), Calcite ($CaCO_3$), Rulite (TiO_2), Sodium aluminium silicate ($Na(AlSiO_4)$), Gibbsite ($Al(OH)_3$) and Goethite (FeO(OH)). Phase identification was performed by qualitative peak matching using the ICDD database within X'Pert HighScore software, and Rietveld refinement was not applied, as the XRD analysis was intended to provide qualitative phase identification rather than quantitative phase analysis for the multiphase red mud–filled polypropylene composites. [27]. In the XRD

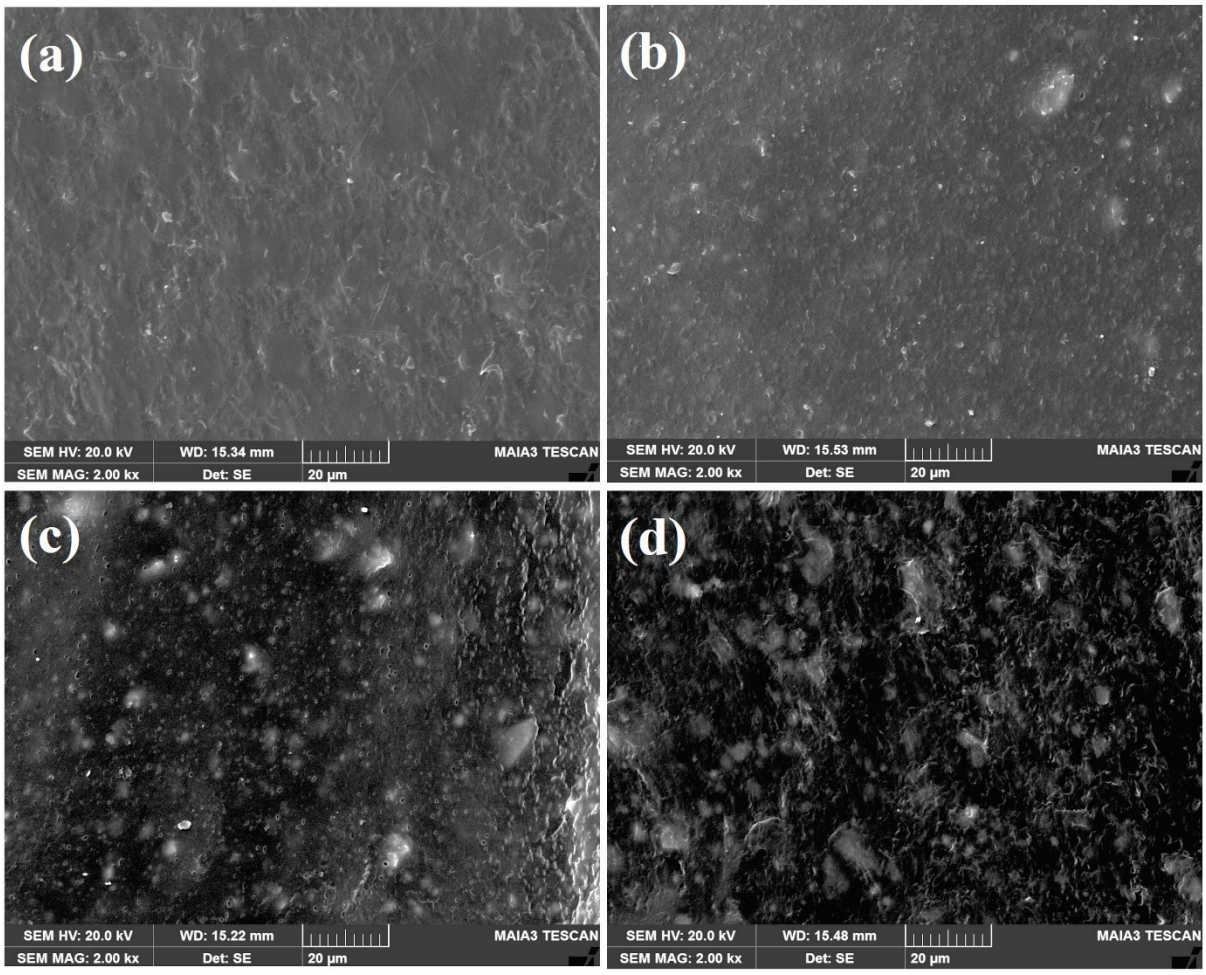

Figure 3. SEM images of (a) pure PP, (b) 10 wt%, (c) 30 wt%, (d) 40 wt% red mud powder mixed PP composites.

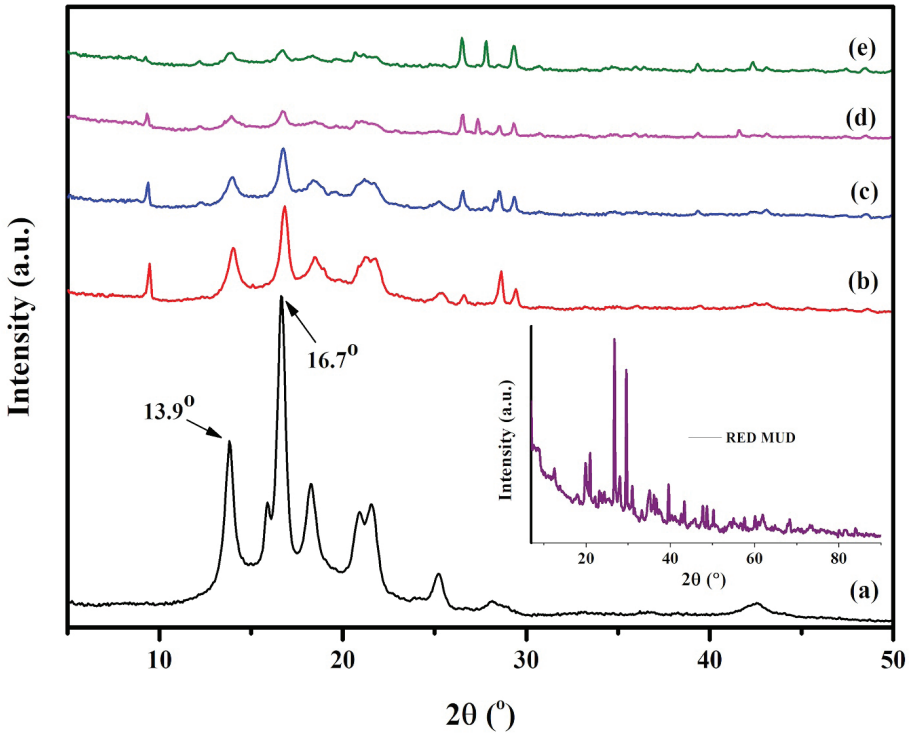

Figure 4. XRD patterns of (a) pure PP, (b) 10 wt%, (c) 20 wt%, (d) 30 wt%, (e) 40 wt% red mud powder mixed PP composites.

pattern of the PP matrix given in Figure 4a, two different crystal planes given in the literature were observed in 2θ of 13.9° and 16.7° [28].

Upon analysis of the pattern, it was observed that the addition of red mud (RM) led to an increase in the crystallization degree of polypropylene (PP). The intensity of the PP peaks decreased as the ratio of RM mixed with PP increased. New peaks appeared in the spectrum due to the mineral substances in the red mud. It is known that the crystalline nature of the thermoplastic polymer affects its thermal properties, and thus, modifying the crystallization process can improve its thermal properties [29-31]. After XRD measurement, the percentage of crystallinity of red mud-reinforced polypropylene composites was determined using the following equation [32]:

$$Percent\ Crystallinity = \frac{I_{crystalline}}{I_{crystalline} + I_{amorphous}} \times 100 \quad (1)$$

From the results obtained using Equation 1, the percentage of crystallinity increased with increasing red mud content. The percent crystallinity were 90,29% for RM, 80,04% for PP, 80,18% for 10.0 wt% PP/RM composite, 83,75% for 20.0 wt% PP/RM composite, 87,34% for 30.0 wt% PP/RM composite and 94,94% for 40.0 wt% PP/RM composite (Fig. 5).

The material's crystallinity increased proportionally with the increasing concentration of highly crystalline RM in the matrix. This relationship is reinforced by the detection of an increasing number of new peaks in the XRD spectrum as the RM ratio increases, indicating a higher degree of crystallinity.

Dynamic Mechanical Analysis

Figure 6 compares storage modulus against temperature for pure polypropylene (PP), and PP compounded with 10 wt.%, 20 wt.%, 30 wt.%, and 40 wt.% red mud (RM). The storage modulus (E') of the RM-doped composites was lower than that of pure PP at lower temperatures. At 25°C, E' of pure PP was measured at 6.28 x 10^8 Pa. However, the composite with 40 wt.% RM showed a storage modulus of only 2.60 x 10^8 Pa at the same temperature, representing a 58% decrease. This reduction is likely due to the increased agglomeration of red mud particles within the polypropylene matrix. As the filler loading increases, particle-particle interactions become more dominant than particle-matrix interactions [33,34]. The agglomeration reduces the efficiency of stress transfer between the matrix and the filler. Also, the lack of a compatibiliser or surface treatment weakens interfacial adhesion. This heterogeneous dispersion reduces stiffness.

Thermogravimetric Analysis

PP is a polymer with low thermal stability. This feature limits its application areas. PP is mixed with various additives to improve its thermal properties. This study aimed to

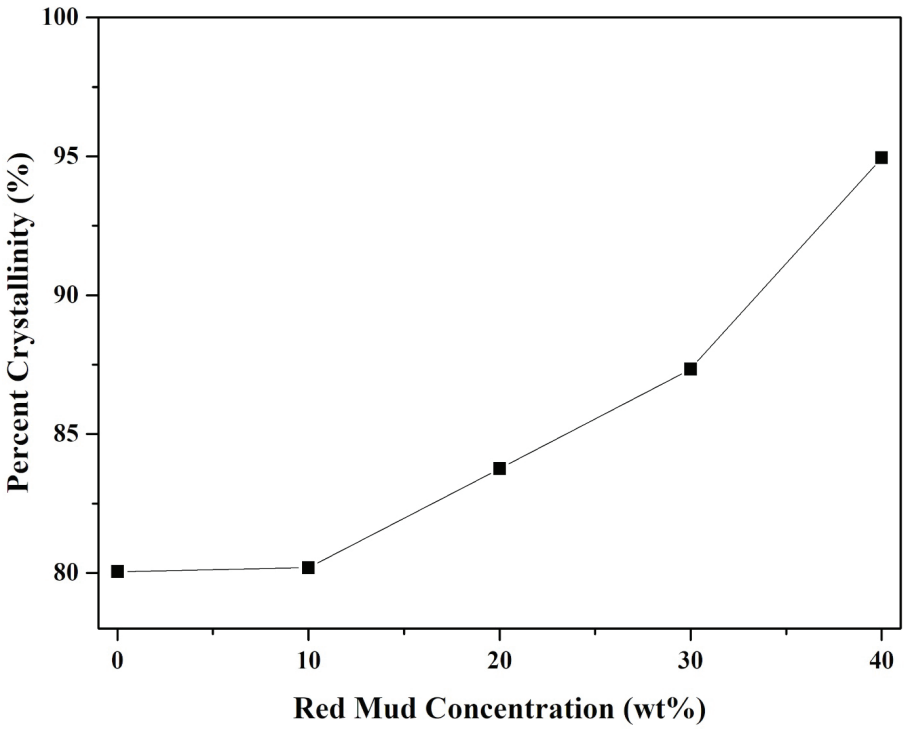

Figure 5. Percent crystallinity depending on red mud content (0, 10, 20, 10, and 30 wt%).

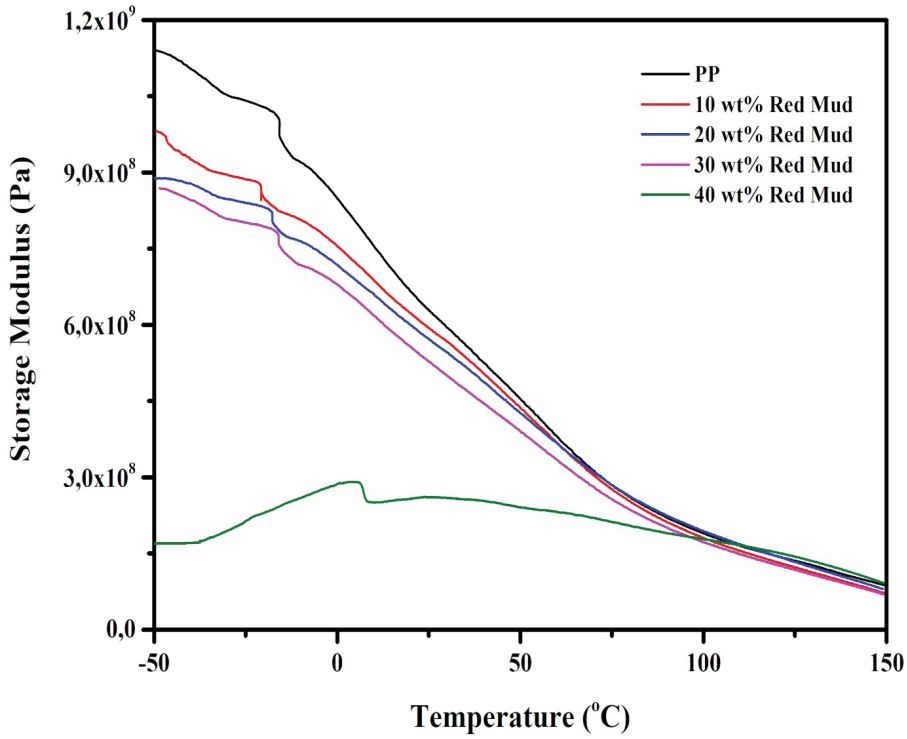

Figure 6. Storage modulus of PP/RM composites containing varying amounts (0-40 wt%) of red mud powder.

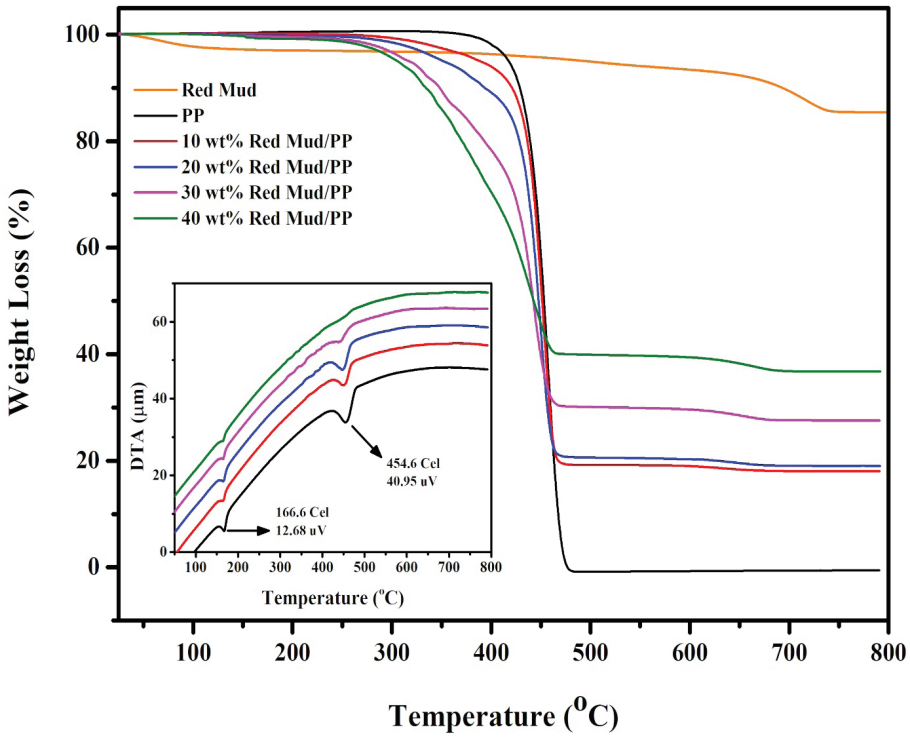

Figure 7. TGA thermograms of RM and PP/RM polymer composites with different percentages (0-40 wt%) of red mud powder.

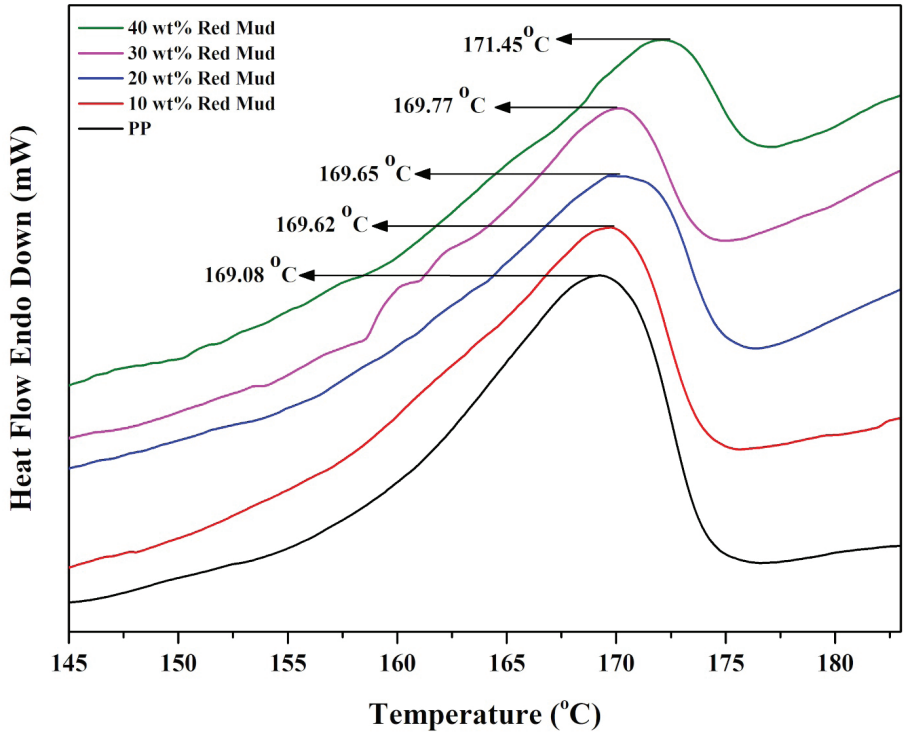

Figure 8. DSC measurement results of PP/RM polymer composites with different percentages (0-40 wt%) of red mud powder.

enhance PP's thermal stability by incorporating red mud, a low-cost waste material. Thermal behaviour of the RM, pure and 10 wt.%,20 wt.%, 30wt.% and 40 wt% red mud mixed PP matrix is shown in Figure 7. For RM, the 2.98% mass loss observed up to 200 °C is attributable to the loss of physically adsorbed water. The 3.62% mass reduction within the temperature interval of 200-600 °C is a result of the dehydroxylation of the FeO(OH) and AlO(OH) phases in the RM. The 7.98% mass reduction observed at temperatures up to 800 °C can be attributed to the degradation of the sodalite group in RM [35]. According to the TGA curve of PP, it's clear that all the mass loss occurs suddenly within a specific temperature range, between 374 °C and 476 °C. Incorporating red mud into PP resulted in mass degradation in two steps. Between 25 °C and 800 °C, the mass degradation of the composite decreased with increasing red mud ratio. With increasing temperatures spanning 200-500 °C, weight losses were 80.8% for 90wt/10wt composite, 79.32% for 80wt/20wt composite, 69.73% for 70wt/30 wt% composite and 59.96% for 60wt/40wt composite. Within 500-700 °C, weight losses were 1.14% for 90wt/10wt composite, 1.6% for 80wt/20wt composite, 2.68% for 70wt/30wt composite and 3.22% for 60wt/40wt composite. When measured between room temperature and 800 °C, the 60 wt/40 wt composite exhibited excellent thermal stability, as it showed the lowest mass loss. The TGA results unambiguously indicate that incorporating red mud significantly enhances the thermal stability of polypropylene [36,37].

Differential Scanning Calorimetry Examination

Figure 8 shows the DSC melting curves for pure PP and PP/RM composites with different mixing ratios. The melting temperatures (T_m) of all samples (pure PP, 10 wt.%, 20 wt.%, 30wt.%, and 40 wt% red mud mixed PP matrix) were 169.08, 169.62, 169.65, 169.77 and 171.45 °C, respectively. The Tm of the PP matrix shifted to higher temperatures after mixing with RM, indicating that PP and RM mix well and interact.

CONCLUSION

This study lies in the systematic evaluation of untreated red mud, an industrial waste by-product, as a filler in polypropylene composites without the use of surface modification or compatibilizers. Unlike most previous studies that focus on chemically treated red mud or dispersion-optimized systems, this work provides a direct assessment of the intrinsic effect of raw red mud on the morphological, mechanical, and thermomechanical properties of PP composites.The different crystal structures and mechanical properties of RM influenced the PP-based composites' thermal and dynamic mechanical properties. SEM images revealed agglomeration with increased RM content. At 25 °C, the storage modulus of pure polypropylene is 6.28×10^8 Pa, whereas it decreases to 2.60×10^8 Pa for the 60 wt/40 wt composite. There is a reduction of about 58%. DMA results suggested that the decreased storage modulus of the composites was due to this agglomeration. FTIR analysis confirmed that the composites comprised PP and red mud. The intensity of the PP peaks decreased with increasing RM ratios, whereas new peaks appeared in the spectrum due to red mud. The percentage of crystallinity increased with RM mixed into the matrix, as evidenced by new peaks in the XRD pattern. According to X-ray tests, crystallinity increases from 80.04% for pure polypropylene to 94.94% for the 60 wt/40 wt composite. The melting temperature rises slightly from 169.08 °C to 171.45 °C as red mud content increases. The shift of Tm to higher temperatures in the DSC result indicated a good mixing of RM with PP. Thermogravimetric analysis indicates the composites are more thermally stable, with less mass loss. The 60 wt/40 wt composite exhibits the lowest mass loss up to 800 °C. TGA results demonstrated that low-cost red mud improved the thermal properties of PP, although it exhibited low thermal stability. These results suggest that untreated red mud can be an effective, low-cost filler for polypropylene composites for engineering applications.

From an economic standpoint, utilizing waste materials can help to create new industries and business opportunities while also reducing costs associated with waste disposal. Overall, the utilization of waste materials has the potential to be a win-win for both the environment and the economy. These results suggest that untreated red mud can be an effective, low-cost filler for polypropylene composites for engineering applications.

ACKNOWLEDGMENTS

Thanks to Yıldız Technical University, Science and Technology Application and Research Center, Bartın University Central Research Laboratory and Application Center for enabling the use of the lab equipment and facilities. The authors are also grateful to Marmara University for providing laboratory facilities.

AUTHOR CONTRIBUTIONS

All authors contributed equally to both the research implementation and the manuscript preparation. All authors have accepted responsibility for the entire content of this submitted manuscript and have approved the submission.

DATA AVAILABILITY STATEMENT

All data are included in this manuscript.

CONFLICT OF INTEREST

There is no any conflict of interest.

ETHICS

There are no ethical issues with the publication of this manuscript.

STATEMENT ON THE USE OF ARTIFICIAL INTELLIGENCE

Artificial intelligence was not used in the preparation of the article.

REFERENCES

[1] Swain B, Akcil A, Lee JC. Red mud valorization an industrial waste circular economy challenge; review over processes and their chemistry. Crit Rev Environ Sci Technol 2022;52:520–570. [CrossRef]

[2] Akcil A, Akhmadiyeva N, Abdulvaliyev R, Meshram A, Meshram P. Overview on extraction and separation of rare earth elements from red mud: Focus on scandium. Miner Process Extr Metall Rev 2018;39:145–151. [CrossRef]

[3] Kucukdogan N, Aydın L, Sutcu M. Theoretical and empirical thermal conductivity models of red mud filled polymer composites. Thermochim Acta 2018;665:76-84. [CrossRef]

[4] Yılmaz VM. Altın ve bakır sektöründe atık yönetimi. In: Çevresel Açıdan Sektörel Atık Yönetimi ve Uygulamaları III. Ankara: Nobel Akademik Yayıncılık; 2024. p. 121–144.

[5] Yan P, Chen B, Haque MA, Liu T. Influence of red mud on the engineering and microstructural properties of sustainable ultra-high performance concrete. Constr Build Mater 2023;396:132404. [CrossRef]

[6] Wu P, Liu X, Zhang Z, Wei C. Properties of red mud-filled and modified resin composites. Constr Build Mater 2023;409:133984. [CrossRef]

[7] Liu Z, Yang Y, Xie M, Cheng M, Yang R, Huang Z, et al. TG-FTIR-Py-GCMS analysis and catalytic pyrolysis mechanism of textile waste by red mud catalyst for liquid fuel production. Sci Total Environ 2024;952:175874. [CrossRef]

[8] Uysal M, Kuranlı ÖF, Aygörmez Y, Canpolat O, Coşgun T. The effect of various fibers on the red mud additive sustainable geopolymer composites. Constr Build Mater 2023;363:129864. [CrossRef]

[9] Yin H, Liu J, Zhou X, Qi H, Liu S, Pang S. Flexural properties of fiber-reinforced alkali slag-red mud geopolymer. Constr Build Mater 2023;370:130708. [CrossRef]

[10] Mian MAA, Taotao S, Min D, Wentao X, Yuchen Y, Imran A, et al. Technologies for recovery of iron from red mud: Processes, challenges, and opportunities. Sustain Mater Technol 2024;41:e01053. [CrossRef]

[11] Jiahai B, Li C, Du Q, Dong C. Fabrication and properties of self-foamed glass ceramics from red mud and ceramic tile polishing waste. J Sustain Metall 2024;10:1559–1571. [CrossRef]

[12] Niu A, Lin C. Trends in research on characterization, treatment and valorization of hazardous red mud: A systematic review. J Environ Manage 2024;351:119660. [CrossRef]

[13] Bhat AH, Abdul HPS, KA. Thermoplastic polymer based modified red mud composites materials. In: Attef B, (editor). Advances in Composite Materials - Ecodesign and Analysis. London: IntechOpen; 2011. [CrossRef]

[14] Zhang Y, Zhang A, Zhen Z, Lv F, Chu PK, Ji J. Red mud/polypropylene composite with mechanical and thermal properties. J Compos Mater 2011;45:2811–2816. [CrossRef]

[15] Akıncı A, Akbulut H, Yılmaz F. Mechanical properties of cost-effective polypropylene composites filled with red-mud particles. Polym Polym Compos 2008;16:439–446. [CrossRef]

[16] Ravi Kumar M, Kumar V, Prasad CD, Sridevi G, CR A, Kumar A, et al. Estimating and parametrically improving the microstructure, hardness, and wear resistance of SiC-CeO2 reinforcements on hot rolled Al7075 hybrid composites. Results Eng 2025;26:104634. [CrossRef]

[17] Ravikumar M, Naik R, Vinod BR, Chethana KY, Rammohan YS. Study on nanosized Al2O3 and Al2O3-SiC on mechanical, wear and fracture surface of Al7075 composites for soil anchoring applications. Mater Phys Mech 2023;51:24–41.

[18] Ravikumar M, Chethana KY, Vinod BR, Suresh R. Nano-sized SiC-Gr particulates reinforced AI7075 hybrid composite: Experimental studies and analysis of quenching agents. J Tribol 2023;38:82–99.

[19] Ravi Kumar M, Suresh R. Study on mechanical and machinability characteristics of n-AI2O3/SiC-reinforced AI7075 composite by design of experiment technique. Multiscale Multidiscip Model Exp Des 2023;6:747–760. [CrossRef]

[20] Gümüş BE, Yağci Ö, Taşdemir M. High-density polyethylene/artichoke leaf powder polymer composites: Dynamic mechanical, morphological and thermal properties. Iran Polym J 2022;1:1–11. [CrossRef]

[21] Benli M, Gümüş BE, Kahraman Y, Yağcı Ö, Erdoğan D, Huck O, et al. Thermal, structural and morphological characterization of dental polymers for clinical applications. J Prosthodont Res 2021;65:176–185. [CrossRef]

[22] Gumus BE, Yagci O, Erdogan DC, Tademir M. Dynamical mechanical properties of polypropylene composites filled with olive pit particles. J Test Eval 2019;47:2551–2561. [CrossRef]

[23] Singh S, Aswath MU, Das Biswas R, Ranganath RV, Choudhary HK, Kumar R, et al. Role of iron in the enhanced reactivity of pulverized red mud: Analysis by Mössbauer spectroscopy and FTIR spectroscopy. Case Stud Constr Mater 2019;11:e00266. doi:10.1016/j.cscm.2019.e00266. [CrossRef]

[24] Gotić M, Musić S. Mössbauer FT-IR and FE SEM investigation of iron oxides precipitated from FeSO4 solutions. J Mol Struct 2007;834–836:445–453. [CrossRef]

[25] Christou C, Agapiou A, Kokkinofta R. Use of FTIR spectroscopy and chemometrics for the classification of carobs origin. J Adv Res 2018;10:1–8. [CrossRef]

[26] Al Bakri Abdullah MM, Hussin K, Bnhussain M, Ismail KN, Yahya Z, Razak RA. Fly ash-based geopolymer lightweight concrete using foaming agent. Int J Mol Sci 2012;13:7186–7198. [CrossRef]

[27] Nath H, Sahoo A. A study on the characterization of red mud. Int J Appl Bio-Engineering 2014;8:1–4. [CrossRef]

[28] Alonso M, Velasco JI, De Saja JA. Constrained crystallization and activity of filler in surface modified talc polypropylene composites. Eur Polym J 1997;33:255–262. [CrossRef]

[29] Labour T, Gauthier C, Séguéla R, Vigier G, Bomal Y, Orange G. Influence of the β crystalline phase on the mechanical properties of unfilled and CaCO3-filled polypropylene. I. Structural and mechanical characterisation. Polymer 2001;42:7127–7135. [CrossRef]

[30] Velasco JI, Morhain C, Martinez AB, Rodriguez-Peréz MA, De Saja JA. The effect of filler type, morphology and coating on the anisotropy and microstructure heterogeneity of injection-moulded discs of polypropylene filled with aluminium and magnesium hydroxides. Part 1. A wide-angle X-ray diffraction study. Polymer 2002;43:6805–6811. [CrossRef]

[31] Akinci A, Akbulut H, Yilmaz F. The effect of the red mud on polymer crystallization and the interaction between the polymer-filler. Polym Plast Technol Eng 2007;46:31–36. [CrossRef]

[32] Yağci Ö, Eker Gümüş B, Taşdemir M. Thermal, structural and dynamical mechanical properties of hollow glass sphere-reinforced polypropylene composites. Polym Bull 2021;78:3089–3101. [CrossRef]

[33] Mothé CG, Monteiro DFJ, Mothé MG. Dynamic mechanical and thermal behavior analysis of composites based on polypropylene recycled with vegetal leaves. Mater Sci Appl 2016;7:349–357. [CrossRef]

[34] Zhang J, Sun C, Li P, Ming L, Jiang H, Yao Z. Experimental study on rheological properties and moisture susceptibility of asphalt mastic containing red mud waste as a filler substitute. Constr Build Mater 2019;211:159–166. [CrossRef]

[35] Kazak O, Eker YR, Akin I, Bingöl H, Tor A. Green preparation of a novel red mud@carbon composite and its application for adsorption of 2,4-dichlorophenoxyacetic acid from aqueous solution. Environ Sci Pollut Res 2017;24:23057–23068. [CrossRef]

[36] Reis JML. Fracture and flexural assessment of red mud in epoxy polymer mortars. Mater Struct 2015;48:3929–3936. [CrossRef]

[37] Kazak O, Tor A, Akin I, Arslan G. Preparation and characterization of novel polysulfone-red mud composite capsules for the removal of fluoride from aqueous solutions. RSC Adv 2016;6:86673–86681. [CrossRef]